



Paleomagnetism of trap intrusions, East Siberia: Implications to flood basalt emplacement and the Permo–Triassic crisis of biosphere



Konstantin M. Konstantinov^a, Mikhail L. Bazhenov^{b,*}, Anna M. Fetisova^c,
Mikhail D. Khutorskoy^b

^a Geological Enterprise of Exploration, Diamond Mining Company ALROSA Co. Ltd., Mirny City, Russia

^b Geological Institute, Russian Academy of Sciences, Moscow, Russia

^c Geological Division, Moscow State University, Moscow, Russia

ARTICLE INFO

Article history:

Received 14 November 2013

Received in revised form 12 March 2014

Accepted 13 March 2014

Available online xxxx

Editor: L. Stixrude

Keywords:

Paleomagnetism

Siberian traps

intrusions

brief magmatic pulses

Permo–Triassic mass extinction

ABSTRACT

Despite decades of concentrated studies, large igneous provinces (LIPs) are still among the most enigmatic phenomena of the Earth evolution. Among the myriad questions facing researchers, the duration of eruptive magmatic activity and its distribution through time are probably the most mysterious ones. Although the accuracy of modern dating techniques offers relatively high resolution, it is impossible to discriminate whether magmatic activity was more or less uniform or concentrated in few powerful outbursts. Consequently, many “trap-related” questions, from their origin to possible impact on the biosphere, still cannot be answered. Some of the above questions can be addressed with paleomagnetic data as have been effectively done in the case of the end-Cretaceous Deccan traps. The Siberian traps are one of the largest LIPs in the Phanerozoic and are thought, by some, to be the triggering event for the end-Permian mass extinction. We conducted a paleomagnetic study of trap intrusions along two long profiles in the eastern part of the province and found that most site-mean directions are grouped several times tighter than is common for the data on thick lava series and dyke swarms; similar over-grouping is found in other parts of the Siberian trap province too. We argue that this phenomenon is the most likely related to nearly simultaneous emplacement of trap intrusions over areas of several ten to few hundred kilometers in dimension for few millenniums or even faster. Moreover, such brief events account for all, or nearly all, magmatism in each area; how such events correlate over the entire Siberian LIP, however, remains an open question. Still, our data together with paleomagnetic results on thick lava series in Siberia strongly indicate that magmatic activity consisted of a number of brief pulses. In comparison to the other LIPs, the Siberian one is underlain by the thickest succession of carbonates, evaporites and coal-bearing clastics that are capable of producing huge amount of green-house and poisonous gases. We hypothesize that these very fast injections of magma into thick underlying sediments and the unique geological setting of the Siberian LIP are the major reasons for the Permo–Triassic mass extinction being the strongest in Earth history.

© 2014 Elsevier B.V. All rights reserved.

1. Introduction

Traps, or flood basalts, or large igneous provinces, LIPs, are among the most convincing proofs of our planet being alive and active. Really, these provinces often occupy more than a million square kilometers and their volume often exceeds one million cubic kilometers. So it is not surprising that the swarms of scientists throng over such areas for decades trying to understand how the traps were formed, how they could affect the Earth cli-

mate and biosphere, etc. Many trap-related mysteries would become less mysterious if a definite answer could be found to an apparently simple question: how long did the LIPs form? Two or three decades ago trap volcanism was thought to last many millions years but, due the recent advances in geochronology, its duration is now thought to be about 1 Ma for many LIPs, e.g., Deccan (Chenet et al., 2009) or Siberia (Kamo et al., 2003); moreover, statistical analysis of numerous U–Pb ages has led to conclusion that the Karoo LIP has been formed for about 0.5 Ma (Svensen et al., 2012). Further progress, however, is hampered by a simple fact that age-related errors are usually equal to, or exceed, the duration of trap volcanism. New geochronological data with errors below $\pm 0.02\%$, which corresponds to $< \pm 50$ kyr for the

* Corresponding author.

E-mail address: mibazh@mail.ru (M.L. Bazhenov).

Permian–Triassic boundary, are claimed to be attainable (Burgess et al., 2014), but we know of no example of such data for the LIPs. Without better time constraints, the average rate of trap accumulation that is directly computed by division of the LIP volume by its (assumed) duration is comparable to the present-day volcanic activity, thus jeopardizing the casual relation between trap volcanism and mass extinctions (e.g., Courtillot, 1999). The same reasoning is fully applicable to other models that connect the biosphere crises to gas emanation from thermally affected sedimentary rocks under flood basalts (e.g., Wignall, 2001; Xie et al., 2007; Svensen et al., 2009).

Many features of the geomagnetic field have characteristic times that are comparable to (changes of polarity), or much shorter than (secular variation, polarity transitions), the common accuracy of geochronological data, and several paleomagnetic attempts to disclose the detail of trap volcanism have been undertaken (Mankinen et al., 1985; Chenet et al. 2008, 2009; Moulin et al., 2012; Suttie et al., 2014). The main outcome of these studies is the recognition of large temporal non-uniformity of volcanism, so-called magmatic pulses (Chenet et al., 2008). Note that all such studies are on lava piles, whereas the intrusive trap suites remain nearly unexplored.

Paleomagnetic studies of the Siberian LIP, SLIP (Fig. 1) started more than fifty years ago, but most data had been acquired with outdated methods and cannot be used now. As a result, the number of the studies based on stepwise demagnetization and principal component analysis remains rather limited. The RN and NR polarity sequences were found in thick lava sections in the Norilsk area in the NW corner of the SLIP (NR in Fig. 1; Heunemann et al., 2004) and the Kotuy area in the north of this province (KT in Fig. 1; Pavlov et al., 2011), respectively. These data indicate that trap emplacement encompassed at least three zones (RNR). Magmatic pulses are found in the SLIP too (Pavlov et al., 2011) but cannot be traced laterally over large distances yet. Few other results are on small parts of lava piles (e.g., Pavlov et al., 2007) and cannot be used for evaluating magmatic activity.

Paleomagnetic studies of trap intrusions in Siberia often were of the by-the-way type with few bodies being sampled in addition to a main target (Pavlov and Gallet, 1998). Otherwise, a number of intrusions were sampled from different limited areas for various purposes (Veselovsky et al., 2003; Konstantinov and Gladkov, 2009; Konstantinov et al., 2012), with the data from several such areas being combined sometimes (Veselovsky et al., 2012). Latyshev et al. (2013) performed a more systematic study of trap intrusions in the mid-Angara part of SW Siberia (Fig. 1) and showed that site-mean directions are very tightly grouped over distances up to 200 km, which was attributed to very fast emplacements of huge sills. Still, the number of the data on intrusions is too limited to extrapolate them over the entire SLIP. In this paper, we present new paleomagnetic data on trap-related intrusions that were sampled along two several kilometer long profiles in the eastern part of the Siberian Trap Province. Then, we combine published paleomagnetic data that had been acquired over sufficiently long profiles, analyze the emerging pattern and discuss its bearing on trap emplacement and possible impact of the SLIP on the biosphere.

2. Geological setting and sampling

The Siberian trap province, SLIP, occupies several million square kilometers in the west and north of the Siberian platform, with smaller-scale magmatism along its northern margin (Vasiliev et al., 2000). Borehole and geophysical data indicate that roughly coeval magmatic rocks occupy large areas in the West Siberian basin under the post-Early Triassic sedimentary cover too (Zolotukhin and Al'mukhamedov, 1988). The lava piles are most common in the Tungus (Tunguska) Basin and usually reside on nearly flat-lying

Late Paleozoic terrigenous clastics with coal beds, which gradually wedge out to the Basin margins. Intrusive suites with, locally, minor lava patches surround the flood basalts as a several hundred kilometers wide band (Fig. 1) and may be present at different levels, from the base of the Cambrian evaporites to Upper Permian–Lower Triassic terrigenous rocks (Feoktistov, 1978). Intrusive bodies in boreholes are commonly interpreted as thick sills up to several hundred kilometers in length that are accompanied by dykes and stocks (Vasiliev et al., 2000; Tomshin et al., 2005). More detailed studies (e.g., Korobkov et al., 2013), however, indicate that the “sills” may vary several times in thickness or wedge out altogether over short distances and rather represent the levels of maximum concentration of intrusive bodies.

The SLIP was initially thought to form over several ten Ma (e.g., Feoktistov, 1978) but the later studies narrowed to few Ma (Reichow et al., 2009) or even 1 Ma (Kamo et al., 2003) straddling the Permo–Triassic boundary. Recent studies appear to indicate that the main magmatic stage encompassing >90% of magmatic rocks was followed by a smaller outburst of magmatism ca. 10 Ma later (Ivanov et al., 2013); however, the U–Pb ages on zircons still consistently group around ~250 Ma (Paton et al., 2010). The pattern becomes even more confusing after the appearance of the new Time Scale 2012, which places the base of the Triassic at 252.2 Ma instead of the previous value of 251.0 Ma (Gradstein et al., 2012). Thus there seems to be no compelling evidence on the precise age of Siberian traps and magmatism duration yet.

Our study area is on uplift between the eastern part of the Tungus Basin and northwestern part of the eastward deepening Viluy basin (also often referred to as the Viluy rift). In this region, nearly flat-lying Paleozoic series is locally overlain by a thin veneer of Upper Permian–Early Triassic sediments and lavas that rarely exceed 100 m in thickness, which are in turn covered with several ten meters thick Mesozoic and Cenozoic sediments. Trap sills and dykes of mafic composition intrude into Paleozoic sediments at shallow depth as indicated by petrographic data (Tomshin et al., 2005) and have never been deeply buried since then. Some authors divide the intrusions in this region into four magmatic complexes, about 70% of intrusions belonging to one of them (Tomshin et al., 2005), while others dispute this division and recognize multiple volcanoes and groups of volcanoes, whose cones had been eroded later (Korobkov et al., 2013).

Two sampling profiles were studied. The first one is along a road to the north on the Viluy River (RD in Fig. 1 and Fig. 3a), where samples were taken at 28 sites along a ca. 90 km long segment of this road. The difference in altitudes between sampling sites exceeds 150 m. Dark massive dolerites, often with columnar jointing, were sampled here.

The second profile is the valley of the Ygyatta River (YG in Fig. 1 and Fig. 4a), where twelve sites were taken along ca. 70 km long profile, with the difference in altitudes between the first and last sites about 80 m. The most volcanics here are thought to be a single sill with average thickness of about 100 m that covers an area of 80 km by 40 km at least (Tomshin et al., 2005). Dark massive dolerites, often with columnar jointing, were sampled here.

3. Methods

Samples were taken as hand blocks everywhere and oriented with a magnetic compass. One cubic paleomagnetic specimen from each sample was stepwise demagnetized up to 600 °C in a custom-designed oven with internal residual fields of about 10 nT and measured with Czech JR-4 and JR-6 spinner magnetometers in the Geological Institute in Moscow. Demagnetization results were plotted on orthogonal vector diagrams (Zijderveld, 1967), and linear trajectories were used to determine directions of magnetic components by the least squares fit comprising three

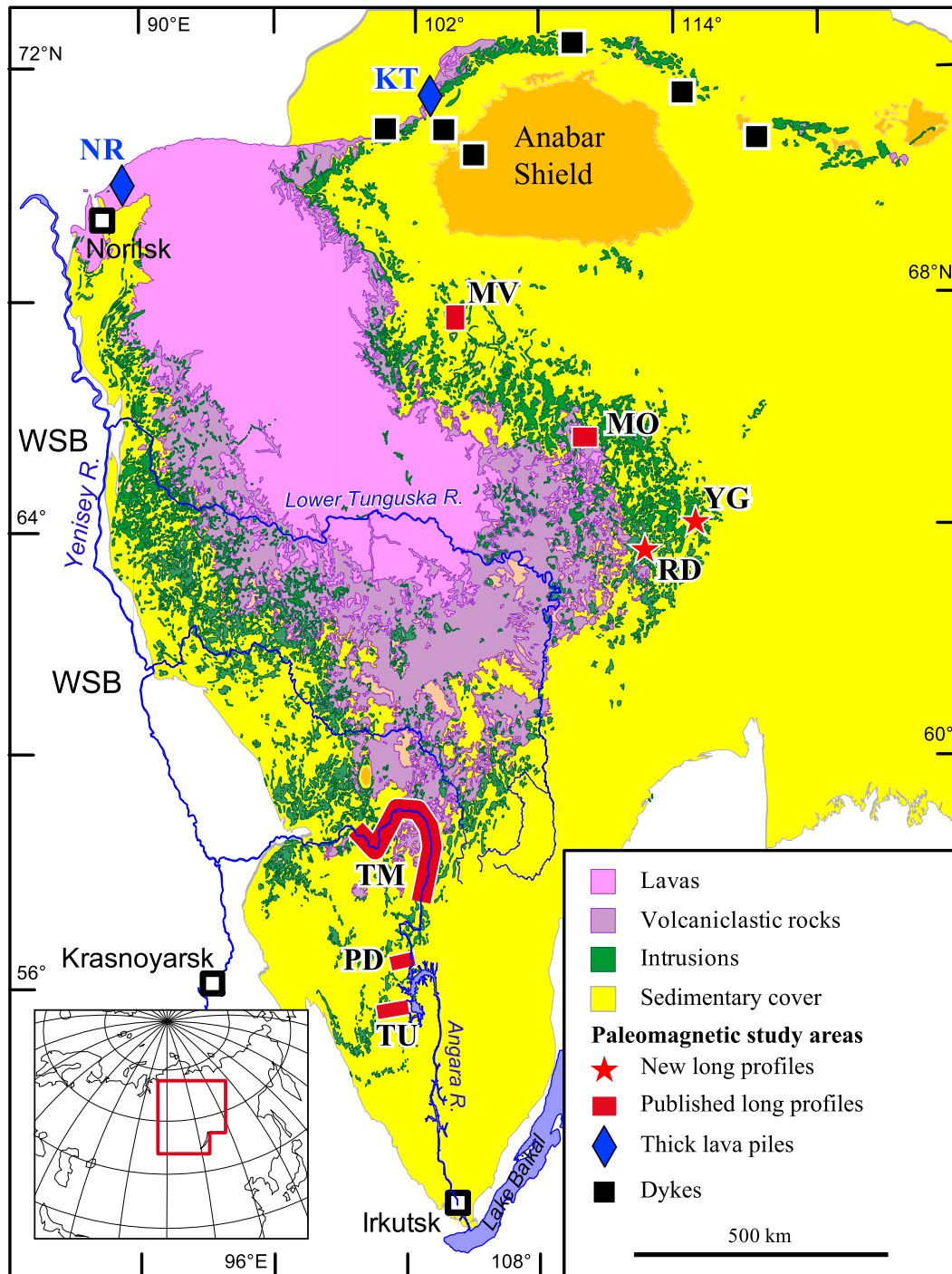


Fig. 1. Map of the Siberian Trap Province (simplified and modified after [Svensen et al., 2009](#)), with a general location map in the lower left corner (the outside frame of the main figure shown as thick line), and paleomagnetic sampling localities labeled as in the text. WSB, the West Siberian basin that is filled with post-Early Triassic sediments.

measurements or more ([Kirschvink, 1980](#)), with anchoring of the fitted lines to the origin where appropriate. Site mean directions were computed either using direct observations (isolated components) or, rarely, combining them with remagnetization circles after [McFadden and McElhinny \(1988\)](#). All site-means are listed in Supplementary data (Tables A1 and A2). Only sites with confidence circles $\alpha_{95} < 15^\circ$ were used for calculation of locality-means. Paleomagnetic software written by Jean-Pascal [Cogné \(2003\)](#) was used in analysis. Rock-magnetic studies were carried out at Petromagnetic Laboratory, the Schmidt Institute of Physics of the Earth and the Borok Geophysical Observatory with the aid of a home-made

two-component thermomagnetometer and automatic coercivitymeter.

As all paleomagnetic directions on the Siberian traps are very steep, mapping them into poles leads to a very scattered distribution of the latter (see Supplement for more detail). Consequently, we performed analysis in directional space and recalculated all data to a common point at 63.5°N , 112.5°E . Published results were used only if they are based on sufficiently large datasets that were subjected to detailed stepwise demagnetization and principal component analysis. Usually, standard angular deviation s that is given by equation $s = 81/(k)^{0.5}$, where k is concentration parameter

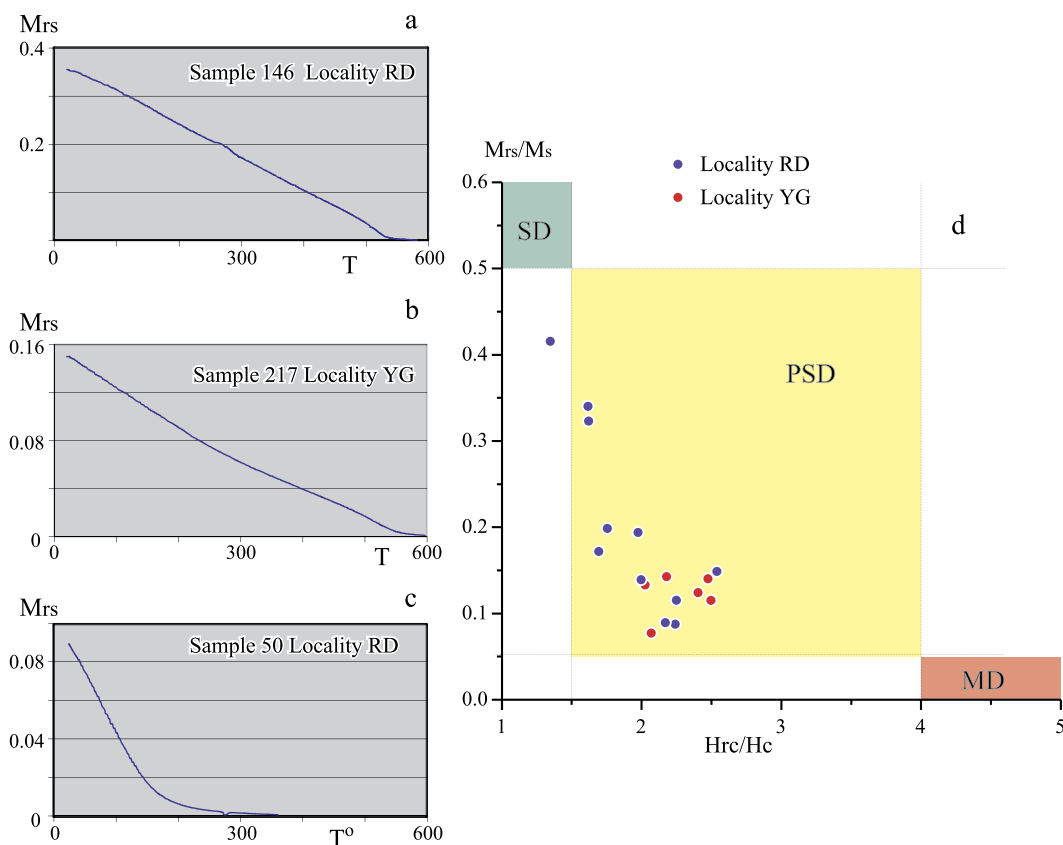


Fig. 2. Results of rock-magnetic studies. (a–c) Plots of remanent magnetization after saturation M_{rs} versus temperature for representative samples from localities RD and YG. M_{rs} values are in A/m; temperatures are in degrees centigrade. (d) Plot of hysteresis parameters (Day et al., 1977), which indicates domain states (SD = Single Domain, PSD = Pseudo-Single Domain, MD = Multi Domain) of the samples from localities RD and YG (blue and red symbols, respectively). M_s = induced saturation magnetization, M_{rs} = remanent magnetization after saturation, H_c = coercivity, and H_{rc} = coercivity of remanence. (For interpretation of the references to color in this figure legend, the reader is referred to the web version of this article.)

(Fisher, 1953), is used for analysis of paleomagnetic data. Because of several reasons (see Supplement), k values were used here for the same purpose. Finally, paleomagnetic datasets are usually compared with the aid of general parameters. We complement this approach with visualizing the distributions by drawing circles that include a large percentage (95% or 99%) of unit vectors (see Supplement).

4. Results

4.1. Rock magnetic introduction

Rock magnetic properties of trap intrusions at both localities showed that the main remanence carrier is low-Ti titanomagnetite or pure magnetite with Curie temperatures in the 550 °C–580 °C range (Fig. 2a, b). A study of hysteresis parameters shows all the data fall in the pseudo-single domain (PSD) field (Fig. 2d). The above, however, is valid only for the samples where a stable component of remanent magnetization was successfully isolated with the aid of thermal demagnetization. In contrast, a magnetic mineral with unblocking temperatures between 200 °C and 300 °C (Fig. 2c), probably high-Ti titanomagnetite, prevails in samples where no stable component was detected.

A similar pattern was discovered in other trap rocks, both lava flows and intrusions (Heunemann et al., 2004; Gurevitch et al., 2004). In most cases, the main remanence carrier is low-Ti titanomagnetite or pure magnetite with Curie temperatures in the 500 °C–580 °C range. Hematite and pyrrhotite are rare.

4.2. Viluy River locality (RD)

A low-temperature component of natural remanent magnetization, NRM, of variable magnitude is present in most samples from all sites and is removed by heating to 200 °C–300 °C. Its directions show some concentration to the present-day field direction, but grouping is poor. This component is likely a mixture of a recent viscous remanence and a spurious one that was acquired during sample handling. As such, these data convey no useful information and are not used further.

Some samples or even entire sites lose >90% of the NRM after heating to 200 °C–300 °C, and no consistent pattern can be found after that (Fig. 3b). Most samples, however, reveal a well-defined component above 300 °C that shows the rectilinear decay to the origin and may be of different polarity (Fig. 3c–e). The site-means that are based on too few samples ($n \leq 3$) and/or have poorly defined site-mean directions ($\alpha_{95} > 15^\circ$) are rejected, while accepted site-means form two nearly antipodal clusters (Fig. 3f, Table 1A). At the same time, concentration parameter values for reverse and normal data differ greatly ($k = 27.4$ and $k = 128.9$, respectively, Table 1). Unfortunately, no cross-cutting relationship between normally and reversely magnetized bodies is found here, and we cannot establish their succession. A comparison with the data on thick lava series does not help either, as the polarity patterns in the Norilsk (Heunemann et al., 2004) and Kotuy (Pavlov et al., 2011) areas are different.

4.3. Ygyatta locality (YG)

On the whole, the low-temperature component here is much weaker than at the previous locality, and a well-defined compo-

Table 1
Summary of paleomagnetic directions in trap-related intrusions of Siberia and high-latitude PSVL data on other objects

#	Objects	Slat (°N)	Slon (°E)	Age	L (km)	A (m)	N	D (°)	I (°)	k	α_{95} (°)	POL	GR	REF
Trap intrusions in Siberia														
1	RD-N	63.4	112.5	251	~80	>150	13	102.1	82.6	129	3.7	N	TI	TP
2	RD-R	63.4	112.5	251	~80	>150	6	335.7	-78.2	27	13.0	R	DI	TP
3	YG	64.0	115.0	251	~70	~80	12	266.4	-83.0	108	4.2	R	TI	TP
4	MO	65.5	110.5	251	~35	~50	9	24.8	76.9	171	3.9	N	TI	1
5	MV	67.6	104.1	251	>80	120	9	83.2	81.5	158	4.1	N	TI	2
6	TM	58.6	101.6	251	>200	n/r	38	149.7	86.6	277	1.4	N	TI	3
7	PD	56.2	101.6	251	~45	n/r	6	302.3	-80.9	646	2.6	R	TI	3
8	TU	55.1	101.1	251	~45	n/r	9	263.7	-62.9	73	6.1	R	QU	3
9	AN	~57	~101	251	>300	n/a	9	146.7	80.6	27	10.1	NR	DI	3
10	DY	n/a	n/a	251	n/a	n/a	44	71.7	80.8	33	3.8	NR	DI	4
11	Σ DI	n/a	n/a	251	n/a	n/a	59	91.5	82.4	28	3.5	NR	DI	TP
Other Data														
12	NR	70	90	251	n/a	n/a	42	86.1	75.4	68	2.7	NR	QU	5
13	KT*	71.3	102.5	251	n/a	n/a	26	123.7	74.8	66	3.5	NR	QU	6
14	EV	-78	165	<5	n/a	n/a	116	13.2	-80.7	23	2.8	NR	DI	7
15	AC	79	267	95	n/a	n/a	37	284.8	80.1	44	3.6	N	DI	8

Comments. All data on Siberian traps are recomputed to the common point at 63.5°N, 112.5°E. Entries ## 1–9 are named as in the text; DY, dykes from Northern Siberia; Σ DI, all diffuse data (DI) combined; EV, Erebus Volcano, Antarctica; AC, Arctic Canada; NS, Norilsk area in NW Siberia; KT, Kotuy area, N Siberia. Slat & Slon are mean coordinates of the localities (n/a, not applicable). Age is in Ma. L is the distance in kilometers between the remotest sites in at each locality. A is the maximal difference in altitudes in meters between the sites from a locality (n/r, not reported). N is the number of sites. D is declination. I is inclination. k is concentration parameter. α_{95} is the radius of confidence circle (Fisher, 1953). POL is polarity: N, normal; R, reverse; NR, mixed. GR, data grouping: TI, tight; DI, diffuse; QU, questionable. REF is the reference: TP, this paper; 1, Pavlov et al. (2007); 2, Konstantinov et al. (2007); 3, Latyshev et al. (2013); 4, Veselovsky et al. (2012); 5, Heunemann et al. (2004); 6, Pavlov et al. (2011); 7, Lawrence et al. (2009); 8, Tarduno et al. (2002).

* Statistics is for flows and directional groups as defined in Pavlov et al. (2011).

ment, which shows the rectilinear decay to the origin and is reverse everywhere, is isolated from most samples above 300 °C (Fig. 4b, c). In about 20% of samples, however, three components, reverse, normal, and reverse, appear to be present (Fig. 4d, e). Their directions are nearly antipodal both within each site and the entire collection; for instance, the locality-means for the intermediate-temperature normal component and high-temperature reversed one differ by ~178 °C, i.e. ~2 °C after inversion to one polarity. This pattern is likely due to not to co-existence of three components of different polarities and, hence, of different ages but the self-reversal of natural remanent magnetization, which is rather common in different parts of the SLIP (e.g., Veselovsky et al., 2003). Accordingly, we used the omnipresent highest-temperature component only for statistical analysis. Twelve reverse site-means are tightly grouped, and site Y12 is deviating (Fig. 4f, Tables 1 and A2).

4.4. Other data

We searched for other cases of tight clustering of site-mean vectors from widely spread sites among paleomagnetic data on trap-related intrusions in Siberia. In most cases either the number of sites was too small, or all sites are from very limited areas, a few kilometers in dimensions at most, or both, and hence do not relate; the few published results that satisfy the above two criteria are listed below (Tables 1 and A3 to A6).

Pavlov et al. (2007) sampled eleven sites that are spread over >80 km along the Moyero River, with ~120 m difference in altitudes between the most remote sites (MV in Fig. 1; Fig. 5a). In this dataset, nine normal site-means are tightly grouped, whereas the other two site-means are of opposite polarity (Fig. 5b; Table A3).

Twelve sites were studied part along the ca. 35-km long Morkoka River (MO in Fig. 1; Fig. 5c) with a ~50 m difference in altitudes between the most remote sites (Konstantinov et al., 2007); unfortunately, just three or four pilot samples were studied at some sites. Despite, nine site-means out of ten where a stable remanence was isolated are tightly clustered and one datum is regarded as anomalous (Fig. 5d, Table A4). Still, this case is not a strong one.

An extensive study of trap intrusions was performed in the south-western part of the part of the Siberian LIP along the mid-Angara River (Latyshev et al., 2013). Out of 48 sites spread over >200 km in the northern part of this region (locality TM, Figs. 1 and 5e), 38 site-means of normal polarity form a very tight cluster (Fig. 5f, Table A5).

Trap directions of reverse polarity from a more southern part of the same region are very tightly grouped too (Latyshev et al., 2013), but the limited dimensions and small statistics make this result less convincing (locality PD, Figs. 1 and 5e, g, Tables 1 and A6).

Nine site-means from the southernmost part of this region (Loc. TU, Fig. 1) are claimed to be “excessively” grouped too (Latyshev et al., 2013). Data grouping, however, is less ($k = 72$) than that in the previous datasets (Table 1); besides, the data come from three sub-localities, with three sites in each, and the lateral coverage is thus very uneven. Hence, the TU dataset is not regarded as over-tight here.

Finally, Latyshev et al. (2013) reported a number of site-means that are either from geographically separated places or clearly deviate from the tightly grouped directions. Following these authors, we pooled such data and computed their regional mean (AN in Table 1).

4.5. Summary

We found six cases of paleomagnetic directions on trap intrusions from large areas being tightly clustered ($k > 100$); they are labeled as type TI data in Table 1. Of six TI results, four are of normal polarity and two are reverse. Although TI data clearly predominate at each locality, some “strangers”, outliers or site-means of opposite polarity, are present too. The most complicated is the RD dataset (Fig. 3f), which comprises loosely grouped reverse sites (RD-R) and tightly clustered normal ones (RD-N).

There are two dispersed dataset (RD-R and AN, Table 1). Also dispersed are the results on 62 dykes and sills from several localities (dark squares in Fig. 1) from the northern rim of the Siberian Platform (Veselovsky et al., 2012). They claimed that secular variation of the geomagnetic field, SV, is reasonably well averaged in

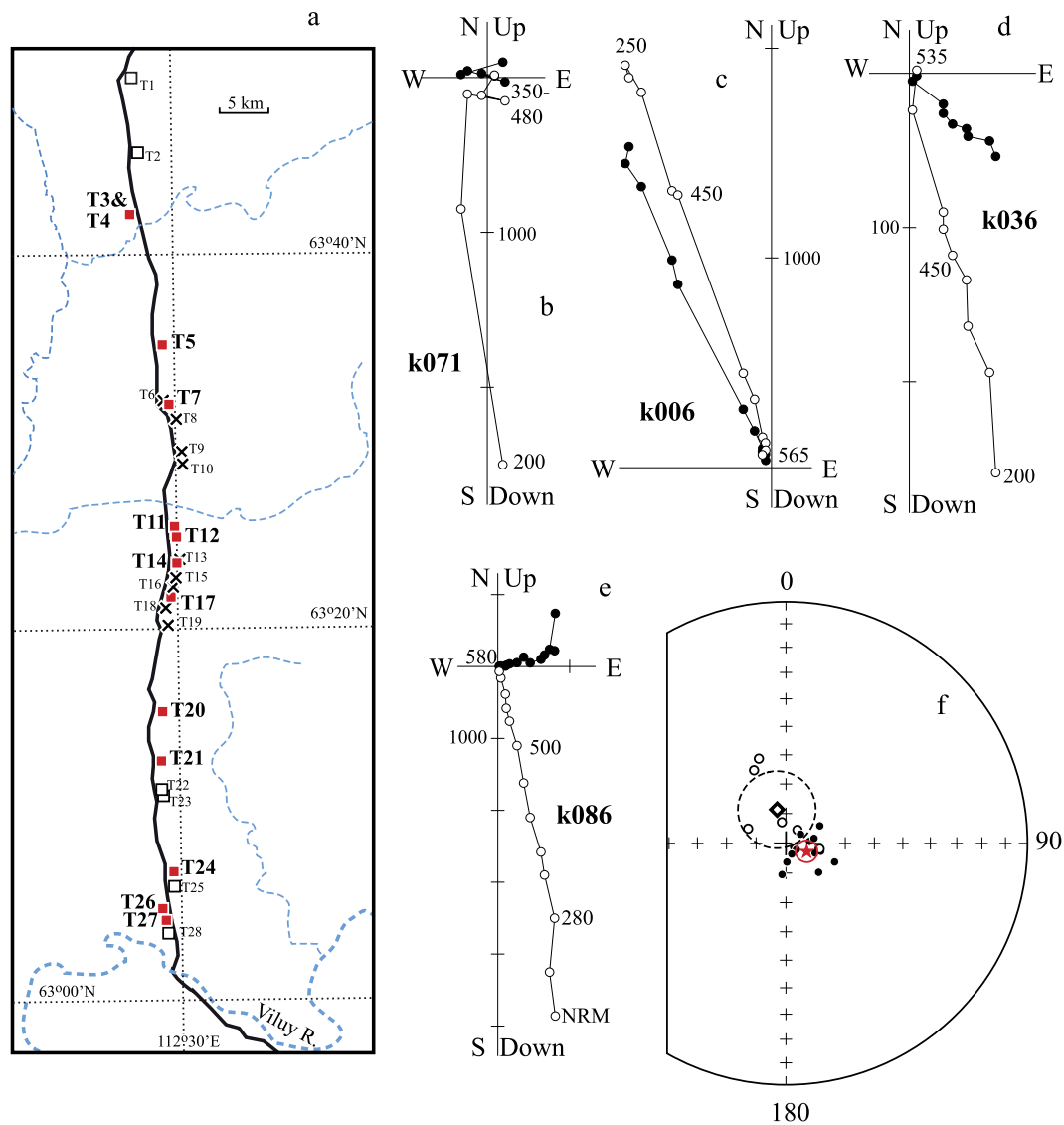


Fig. 3. Sampling area (a) and paleomagnetic results (b–f) on trap intrusions from locality RD. (a) Solid red squares, open squares and oblique crosses denote normally magnetized, reversely magnetized and rejected sites, respectively; the labels for the accepted normally magnetized sites are given in larger characters. (b–e) Representative demagnetization plots of trap rocks in geographic coordinates. Full (open) dots represent vector endpoints projected onto the horizontal plane. Temperature steps are in degrees Celsius. Magnetization intensities are in mA/m. For clarity, NRM points are omitted from some plots. (f) Stereoplots of in situ site-mean directions (circles) of high-temperature components (95% confidence circles for site-means are omitted for clarity) and the overall mean directions for reversely (diamond) and normally (star) magnetized sites with associated 95% confidence circles. Solid (open) symbols and solid (dashed) lines are projected onto the lower (upper) hemisphere. (For interpretation of the references to color in this figure legend, the reader is referred to the web version of this article.)

this dataset, citing in support the presence of both polarities and good agreement of the overall mean pole with the mean trap poles for Siberia (Pavlov et al., 2007); the distances up to ~1000 km between the sampling sites support this view too. We “filtered” the North Siberia dataset by deleting 18 site-means that are based on less than four samples and/or have $\alpha_{95} > 15^\circ$ (DY in Table 1). The comparison of the three dispersed datasets (type DI data in Table 1), however, does not seem to be warranted as RD-R and AN results are based on limited statistics. We are of opinion that the DI data on the whole are best described by combining all DI results (Σ DI in Table 1; Fig. 6a, b).

Thus there appears to be two types of paleomagnetic data on intrusions in the SLIP. One is manifested by tightly grouped directions on magmatic bodies spread over several ten to more than 200 km (TI in Table 1). The data of another type either form much more diffuse distributions (DI in Table 1) or are “strangers” in each area, i.e. single results deviating from the tight groups.

5. Too clustered or too diffuse?

Are the TI data excessively grouped, or are DI ones overly dispersed? To answer this question, we compared the data on intrusive suites with paleosecular variation for lavas, PSVL, data on thick lava series of Siberian traps and other high-latitude objects of various ages (Table 1).

In the Norilsk area (NR in Fig. 1 and Table 1), Heunemann et al. (2004) found few reverse flows at the section base, followed by a thick presumably transitional zone and normally magnetized main part of the section. The data from the latter only were used for computing the locality-mean, but no compelling evidence of adequate SV averaging could be presented (Heunemann et al., 2004). Pavlov et al. (2011) reported a dual-polarity PSVL result on 75 stratigraphically ordered flows from the Kotuy area in the north of the Siberian trap province (KT in Fig. 1 and Table 1). The presence of two polarities and the proximity of the KT pole to the

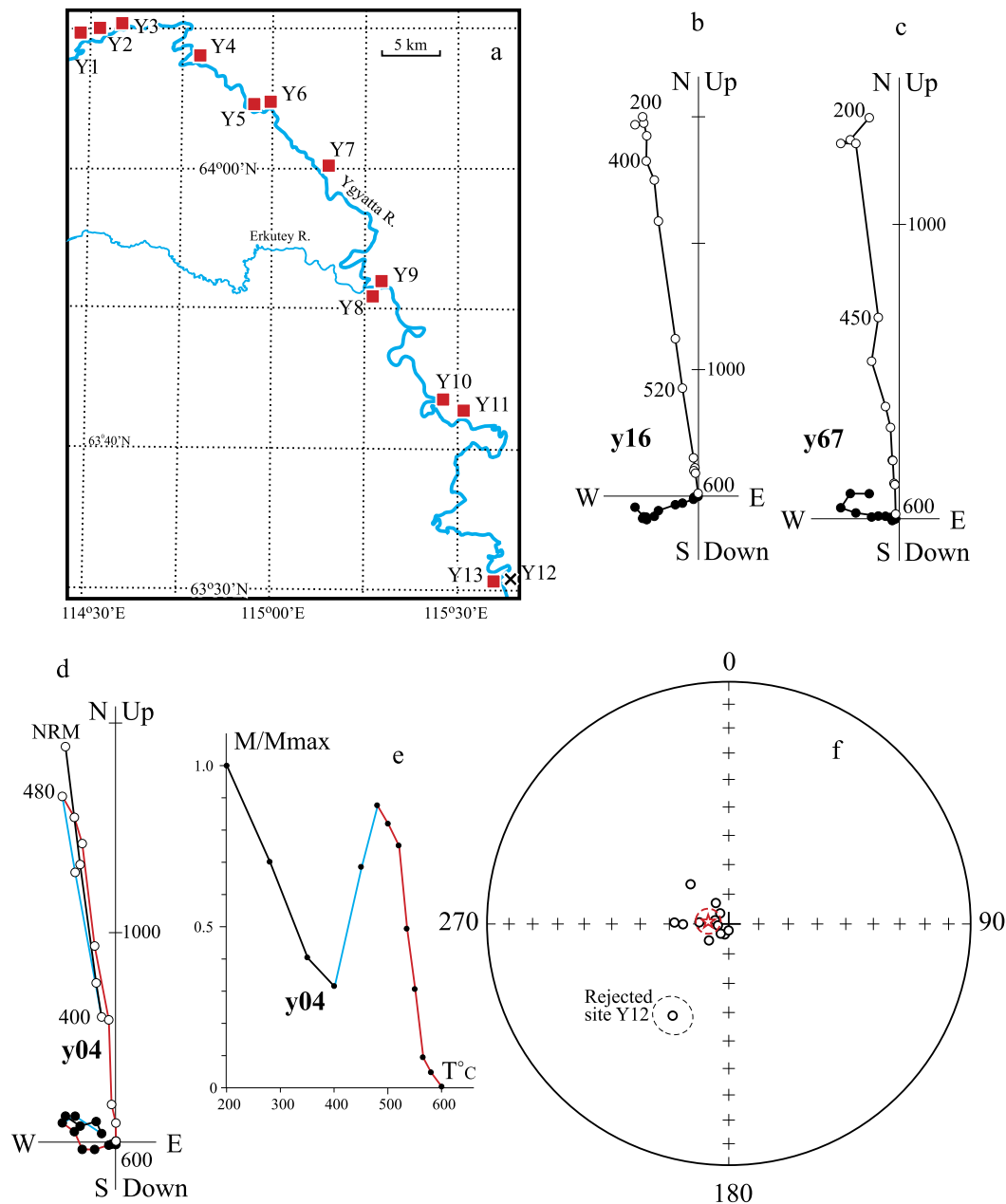


Fig. 4. Sampling area (a) and paleomagnetic results (b–f) on trap intrusions from YG locality. (e) Plot of normalized NRM intensity versus temperature; different segments of this plot and the corresponding orthogonal plot (d) are colored for clarity. (f) Stereoplot of in situ site-mean directions (circles) of high-temperature components and the overall mean direction (star) with associated 95% confidence circle. Other notation as in Fig. 3. (For interpretation of the references to color in this figure, the reader is referred to the web version of this article.)

overall Siberian trap pole are cited by Pavlov et al. (2011) as evidence for adequate SV averaging in the KT dataset. At the same time, the reversal test for the KT dataset is negative, and these authors themselves admit that the SV magnitude may be undervalued.

Regretfully, only two high-latitude ($>60^\circ$) PSVL data of any age that are based on sufficiently large datasets are found (Fig. 7). They are from the Erebus Volcano in Antarctica (Lawrence et al., 2009) and Arctic Canada (Tarduno et al., 2002) (EV and AC, respectively, in Table 1). When all high-latitude data are compared (Table 1), the Σ DI result on Siberian traps well agrees with EV and AC ones, whereas the NR and KT results on thick lava series from Siberia are significantly less dispersed, as evidenced by the statistical tests on concentration parameter values (Table 1; see Supplement for detail). Naturally, all TI data are still tighter. Understanding the vul-

nerability of our decision, we opted for the Σ DI result (Table 1) as the best SV estimate for Siberia by the Permo–Triassic boundary. An additional support for this decision may be drawn from SV models (e.g., Tauxe and Kent, 2004) that, for the latitudes higher than 60° , predict k values of about 25–30, which is close to the Σ DI result. In comparison to this “measuring stick”, the NR and KT data do look as if SV is under-represented, in accordance with the cautionary note by Pavlov et al. (2011). Hence, it is low dispersion of the TI data that calls for explanation.

6. Time–scatter relationship

The SV models (McFadden et al., 1988; Tauxe and Kent, 2004; see Merrill et al., 1996, for other models) and most PSVL data (e.g., Johnson et al., 2008) define a rather narrow range for permissible

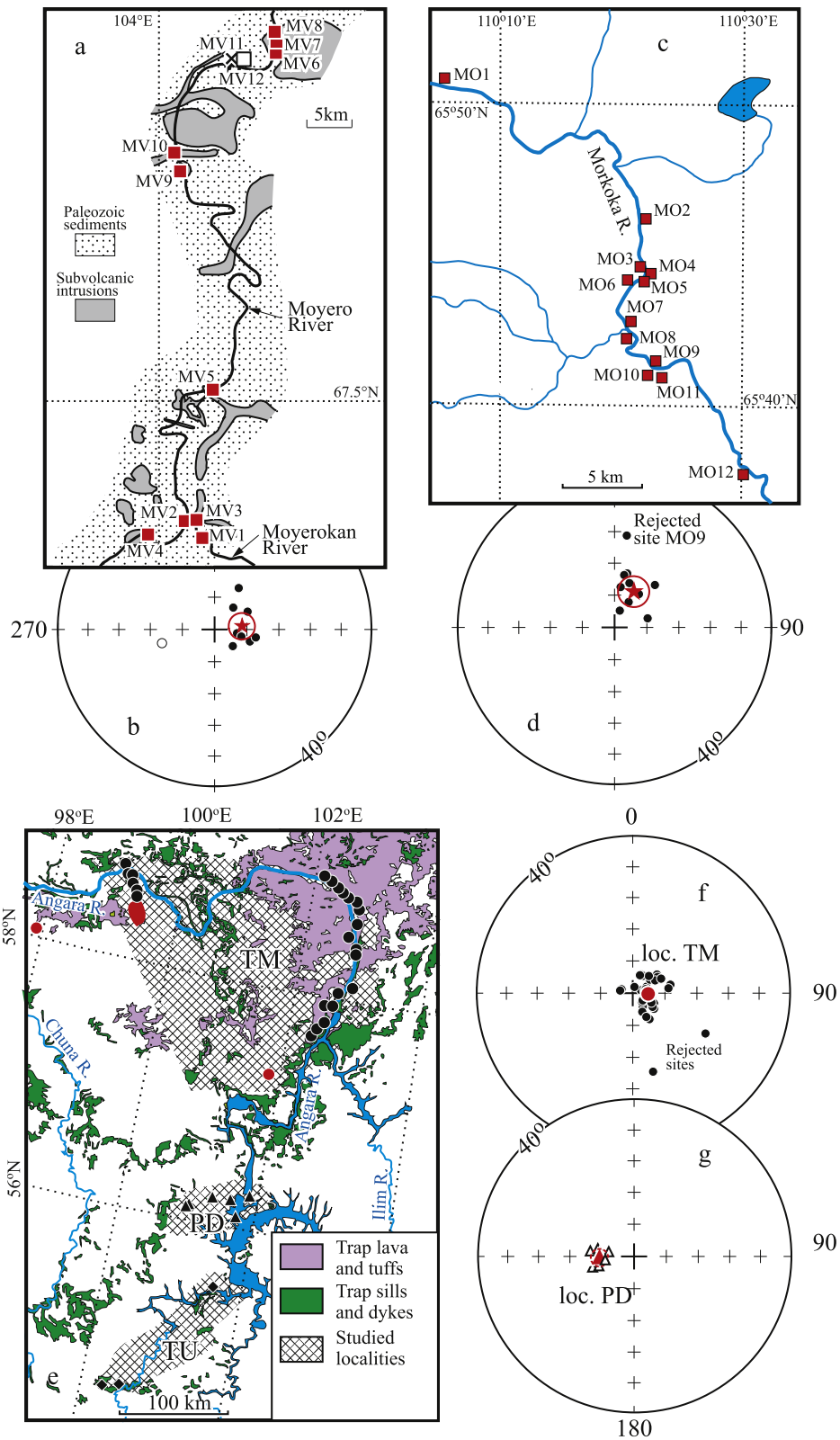


Fig. 5. (a, c, e) Maps of sampling localities and (b, d, f, g) stereoplots of published paleomagnetic data from the other parts of the Siberian traps. (a) Map of locality MV (simplified after Pavlov et al., 2007): solid red squares, open squares and oblique crosses denote normally magnetized, reversely magnetized and rejected sites, respectively. (b) Site-means (circles, confidence circles are omitted for clarity) and locality-mean direction (star) with associated confidence circle (thick line) from locality MV. (c) Location of sampling sites at locality MO. (d) Site-means and locality-mean directions from locality MV. Notation as in (b). (e) Map of the Angara area (simplified after Ivanov et al., 2013 and Latyshev et al., 2013): circles, triangles and diamonds denote the sites from localities TM, PD and TU, respectively. Red spot in the northern part of locality TM and red circles denote the areas where anomalous directions are obtained (see text for detail). (f, g) Site-means (circles, locality TM; triangles, locality PD) and locality-mean directions (larger red symbols). Other notation as in Fig. 3f and (b). All stereoplots are truncated by 40° small circle for clarity. (For interpretation of the references to color in this figure legend, the reader is referred to the web version of this article.)

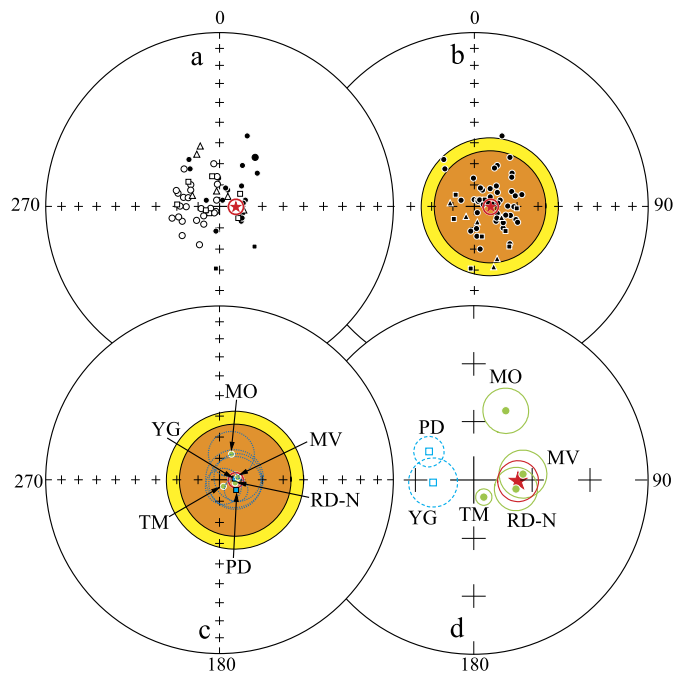


Fig. 6. Stereoplots of (a) the observed site-mean directions from the DY (circles), AN (squares), and RD-R (triangles) dataset (Table 1) and the overall mean direction Σ DI (star) with associated confidence circle α_{95} (thick line). (b) Same but reverse directions are inverted through the origin and filled β_{95} (orange) and β_{99} (yellow) circles are plotted too; (c) α_{95} , β_{95} , and β_{99} from the previous plot are drawn with the locality-mean directions (transformed to normal polarity) and associated β_{95} circles (dotted lines); the means of originally normal (reverse) polarity are shown as circles (squares). (d) Locality-mean directions for TI data and Σ DI vector with associated circles and labeled as on plots (b) and (c) plotted preserving their observed polarity. Note that this stereoplot is zoomed in. All data are recalculated to the common point at 63.5°N , 112.5°E and labeled as in Table 1. Other notation as in Fig. 3f. (For interpretation of the references to color in this figure legend, the reader is referred to the web version of this article.)

k values that do not exceed 50 (Fig. 7). An observed k value in this range does not ensure by itself adequate SV averaging but does not falsify this assumption either. All SV models, however, do not predict how much time is required for SV averaging, or what scatter is to be expected for the data from a certain brief time interval. What we have is the common belief that the data must cover at least 10 kyr for adequate SV averaging and that 100 kyr is always sufficient for this (e.g., Merrill et al., 1996).

The other end-member for the scatter of paleomagnetic data in magmatic rocks is provided by so-called directional groups that are thought to form if lava flows are emplaced over few years to few centuries (Rüsgger et al., 2003). In such groups, k values range from near 100 to >1000 , with most values in the 200–1000 interval; for instance, k values for directional groups of three or more flows are in this range for the KT dataset (blue squares in Fig. 7 from Pavlov et al., 2011) or data from the Deccan traps (Chenet et al., 2008). Note also that the within-site scatter is not taken into account in most papers where such groups are recognized, and the lower limit of the above range is in fact higher.

Hence it is logical to assume that the data covering an interval from few centuries to 10 kyr should produce k values in-between the above limits. A solid support for this conclusion is unlikely to come from geology where even a ten times longer interval is a blink but is provided by archeomagnetic data (Fig. 7). Such data for the western North America for the last 3.5 kyr (Hagstrum and Blinman, 2010) and for France for the last three millennia (Bucur, 1994; Gallet et al., 2002) give k values of ~ 130 and ~ 150 , respectively. Although these data are from the mid-latitudes and of recent age, with reservation, they can be used as proxies. The above data let us assume that the tightly clustered paleomagnetic

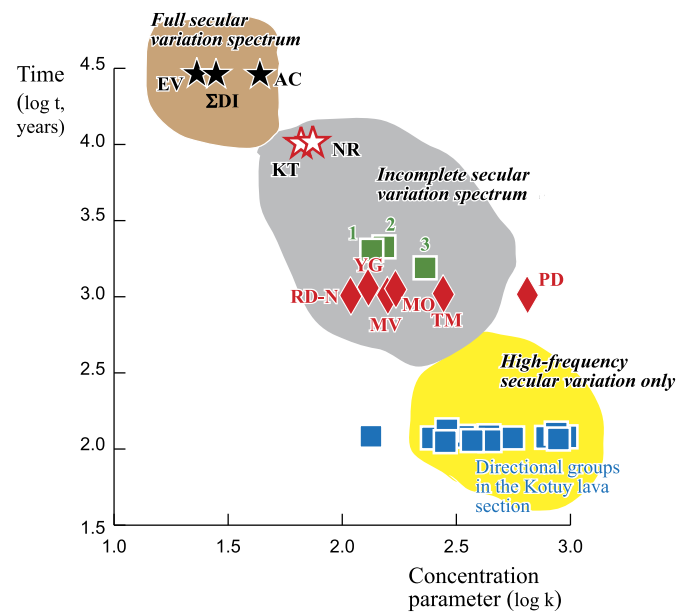


Fig. 7. Schematic cartoon illustrating the relationship between concentration parameter k values for different data types and the duration of time intervals t (in years) that are used for obtaining the data. Note that both axes are on logarithmic scale. Shaded fields are the k - t areas where the full spectrum (brown), incomplete spectrum (gray) and high-frequency only (yellow) of secular variation (SV) is expected. The symbols are keyed as in Table 1: black stars, SV is averaged; white stars, lava sections from NW Siberia; green squares, archeomagnetic data from (1) western North America for the last 3.5 kyr (Hagstrum and Blinman, 2010), (2) France for the last 3 kyr (Bucur, 1994; Gallet et al., 2002) and (3) France for the 1000–0 yr BC interval (Gallet et al., 2002). Blue symbols are the k values for directional groups in the Kotuy dataset (Pavlov et al., 2011). (For interpretation of the references to color in this figure legend, the reader is referred to the web version of this article.)

directions (TI in Table 1) could have been acquired over time intervals of few millennia; perhaps, the most tightly grouped PD data (Table 1) may cover a still briefer time interval (Fig. 7).

Summarizing, we would like to repeat the main results:

1. The formation of intrusive suites with tightly grouped paleomagnetic directions (TI type data) covered at least two polarity zones;
2. SV magnitude is best represented by the pooled DI type data (Σ DI in Table 1);
3. SV is likely under-represented in the lava series studied by Heunemann et al. (2004) and Pavlov et al. (2011);
4. SV is definitely under-represented in the TI datasets, and such level of dispersion matches what is expected for geomagnetic field directions averaged over few millennia at most.

7. Interpretation and implications

Tight clustering of paleomagnetic data occurs if remanence acquisition takes place over time intervals that are either much longer or much shorter than the SV characteristic time of ~ 10 kyr (Merrill et al., 1996). The former case may take place if the deeply buried rocks were uplifted and slowly cooled down. The study area, however, has never been buried more than a couple of hundred meters since the Early Triassic. Otherwise, tightly grouped paleomagnetic directions are often met in remagnetized rocks as the overprint acquisition takes more time than is required for SV averaging. The presence of both TI and DI data at the same locality (e.g., TM, RD, MV) speaks against a regional remagnetization, while rock-magnetic data do not reveal secondary magnetic minerals. Lower Paleozoic rocks in close vicinity of trap bodies are usually completely overprinted but often retain their primary remanence at distances of several hundred

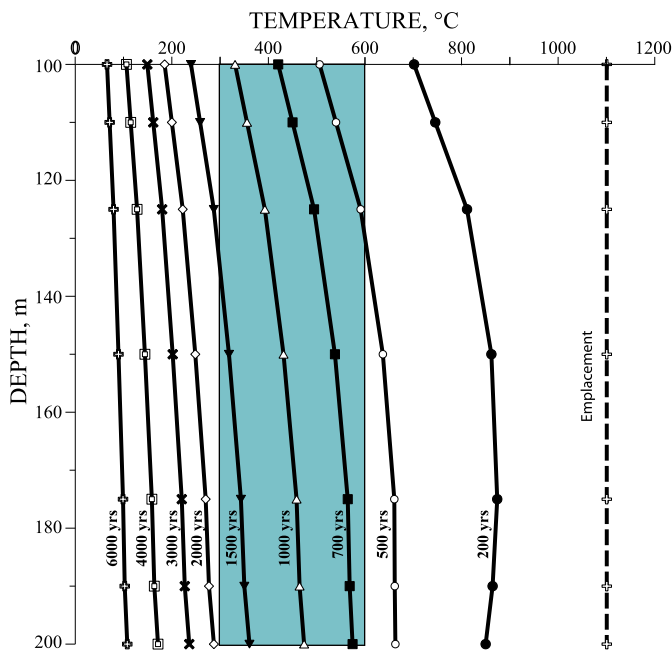


Fig. 8. Cooling history of a 100-m thick basalt sill under 100-m thick cover. Shading corresponds to the interval of remanence acquisition.

meters or more, with the trap remanence being isolated at intermediate temperatures or absent at all (Gallet and Pavlov, 1996; Latyshev et al., 2013). In our opinion, the above data make the overprint hypothesis unlikely.

If remanence acquisition takes place over time interval that is much shorter than the SV characteristic time of ~ 10 kyr, the simplest way to account for the observed pattern is to assume that tightly clustered directions from each area belong to the same intrusion. Geological data apparently indicate that all sampling sites at locality YG belong to a sole 100-m-thick sill with dimensions 80 by 40 km at least (Tomshin et al., 2005). Latyshev et al. (2013) also interpreted their results from localities TM and PD as belonging to just two large sills; in particular, the TM sill is at least 200 km long by 100 km wide with the average thickness of about 200 m (Feoktistov, 1978). The other TI results are from large areas too. Does this mean that each TI datum is from a single thick sill of large lateral extent?

To quantitatively test the single-sill model let us consider a 100-m-thick horizontal sheet of basalt under the 100-m-thick cover. As the injection of liquid magma and its solidification occur much faster than the subsequent conductive cooling of the sill, we assumed that it had had the same temperature of 1100 °C everywhere right after solidification. The characteristic component in trap samples is largely unblocked between 600 °C and 300 °C; consequently, cooling through this interval is what we are interested in. The calculations show that the entire sill could cool from 600 °C to 300 °C in about 1.5 kyr, thus making the single-sill model plausible (Fig. 8). At the same time, the volume of the “small” YG sill is more than 300 km³, whereas the TM sill is about 4000 km³ in volume. In comparison, the largest historic Laki eruption in Iceland when ca. 15 km³ of magma were erupted during several months looks like a molehill. Note in passing that the annual discharges of major rivers like the Rhine or Congo are ~ 80 and 1500 km³, respectively. As the sills were emplaced at a depth that is comparable to their thickness (Tomshin et al., 2005), it is difficult to believe in a Rhine of lava that outflows from a single feeding channel and accurately spreads over large distances under a thin sedimentary veneer within a very limited time span. We simply doubt that this may be common, if possible at all.

Luckily, it does not matter whether one huge sill was emplaced as a single magmatic outburst or many smaller intrusions were injected through multiple feeding channels distributed over a large area during several centuries to few millenniums. In both scenarios, magnetic signatures are similar and are compatible with the formation of the remanence in intrusions for few millenniums at most. Note also that the most intrusions studied belong to the directional cluster at each TI locality, except for loc. RD, where the normally magnetized TI and reverse DI datasets are comparable. Hence it is reasonable to assume that magmatism at each locality consists of a single event of limited duration, with minor but more prolonged activity that resulted in the DI type data.

In turn, it is interesting to see how the TI data are related to each other and to the DI data (Fig. 6c). It is clear that all TI data, both unit vectors and locality-means (plotted together with their β_{95} circles), fall within the DI distribution. The TI data are clearly diachronous as evidenced by the presence of two polarities. The difference of $5.3^\circ \pm 4.0^\circ$ between two reverse means (YG and PD) is small and barely significant; still, it is possible that these two intrusive suites are not exactly coeval. Among the TI data of normal polarity, the TM and MO mean directions are statistically different from the Σ DI mean and each other; hence these intrusive suites are not coeval (Fig. 6d). Finally, the last two normal results (RD-N and MV) are indistinguishable from each other and the Σ DI mean. Note, however, that the data density quickly increases to the center of a Fisher distribution, and the probability of a point falling into the central group by chance is not small. Therefore the close agreement of the RD-N, MV and Σ DI results neither guarantees that the first two suites are coeval nor warrants SV adequate averaging. We are of opinion that the available data are simply insufficient to be sure of this.

Summing up, we conclude that the emplacement of trap intrusions was not a time-distributed process but rather occurred as a single magmatic outburst in many parts of the SLIP. These outbursts were not exactly coeval over the entire trap province, with steadier but much weaker volcanic activity as inferred from the DI type data. Although two models of intrusion formation, that of the single-huge-sill and multiple-brief-intrusive events, cannot be discriminated with available paleomagnetic data, we prefer the latter scenario. If true, this scenario implies that the magma uplift and injection were produced by a set of magma sources that diachronously existed under the SLIP.

Our data on the Siberian trap intrusions have some noteworthy implications to geomagnetism and paleomagnetism. Really, even a large collection from a LIP of, say, 30 sites, which are spread over several tens of kilometers or through thick lava pile, does not ensure that adequate averaging of secular variation is achieved. This imposes important constraints on the reliability of available paleomagnetic data on the flood basalts and sampling policy of the future studies. Unfortunately we cannot compare the Siberian data on trap intrusions with the similar results from other LIPs simply because of the nearly complete lack of the latter, although magmatic suites are common. Paleomagnetic data on few dykes can be found among much more numerous results on lava flows for some LIPs (e.g., Ernesto et al., 1999), but the only (known to us) systematic study of trap intrusions from the Karoo LIP by Hargraves et al. (1997) did not reveal any regular pattern. Hence it remains unknown whether the “Siberian” pattern is a unique feature or simply has not been found in other LIPs yet.

Let’s now recall that over-tight grouping of paleomagnetic data is found at six long profiles from different parts of the SLIP, with the seventh less convincing example of the above-discussed TU area in SW Siberia (Fig. 1). Thus there appears to be enough reasons to assume that vast magmatic pulses are common for the SLIP on the whole. Of course, all studied areas cover just a fraction of

the entire province, and *much* more data are needed to confirm/refute the above assumption.

Three very important facts are to be stressed. First, the SLIP includes both one of the largest lava fields of the world and a still larger area impregnated with multiple intrusions, while intrusive areoles for other LIPs are of smaller dimensions. Second, the Siberian traps overlap a large sedimentary basin of the Tungus Syncline that is filled with Lower-Middle Paleozoic carbonates and evaporites and Carboniferous–Permian terrigenous rocks with abundant coal beds and seams (the Tungus Series). An inspection of other LIPs shows that neither resides on a sediment-filled basin of similar dimensions. Finally, most of the Tungus Syncline filling is capable of producing large amount of green-house and/or poisonous gases like carbon and sulfur dioxides, as has already been stressed by different authors (Wignall, 2001; Xie et al., 2007; Retallack and Jahren, 2008; Svensen et al., 2007, 2009; Ganino and Arndt, 2009; Black et al., 2012). All these studies, however, estimated the net effects only using the imprecisely known total volume and duration of the trap magmatism. The situation resembles that for the Deccan traps, whose ecological impact became much better outlined only after accurate portrayal of history of magmatic activity (Chenet et al., 2009).

Thus we come to the last assumption in this paper: a very important cause, perhaps the major one, of the mass extinction by the Permo–Triassic boundary was intrusion of huge volumes of magma during brief magmatic pulses into thick sedimentary series and producing large quantities of green-house and/or poisonous gases. The unique setting of the SLIP over a basin that is very favorable for massive gas emanation is the reason why the Permian–Triassic event is undoubtedly the strongest among the other biocatastrophes (Rau and Sepkoski, 1982; Erwin et al., 2002). On the other hand, the massive degassing of sedimentary sequences cannot be the only cause of mass extinctions, as evidenced by the Deccan traps that are not underlain by thick sediments. A more detailed analysis of all similarities and dissimilarities between different LIPs and their ecological impacts, however, is out of scope of this paper.

8. Conclusion

We studied trap intrusions along two profiles in the eastern part of the Siberian trap province and found that most site-mean directions are grouped several times tighter than is common for the data on thick lava series and dyke swarms. A similar pattern has recently been reported from the SW part of the SLIP (Latyshev et al., 2013) and also found for two other areas of this province too. Analysis of reliable paleomagnetic data of Siberian traps shows that the magnitude of secular variation of the geomagnetic field by the Permo–Triassic boundary was generally comparable to that at other epochs. Hence the over-tight grouping of paleomagnetic data on trap intrusions is attributed to remanence acquisition spanning several times shorter time intervals than what is presumably requested for representative record of secular variation. We argue that this phenomenon of over-tight grouping is most likely related to nearly simultaneous emplacement of trap intrusions over areas of several ten to few hundred kilometers in dimension for one to three millenniums, or even faster. Moreover, such brief events account for all, or nearly all, magmatism in each area. The data on both trap intrusions and thick lava series in Siberia indicate that magmatic activity consisted of a number of brief pulses, as already shown for huge lava piles for instance in the case of the Deccan traps (Chenet et al., 2009). In comparison to other LIPs, the Siberian one is underlain by the thickest succession of carbonates, evaporites and coal-bearing clastics that are capable of producing huge amount of green-house and poisonous gases (e.g., Svensen et al., 2009;

Ganino and Arndt, 2009). We hypothesize that these huge fast injections of magma into thick underlying sediments and the unique geological setting of the Siberian LIP is the major reason for the Permo–Triassic mass extinction being the strongest in Earth history.

The above statement is a hypothesis that should be further tested. We do not know, however, many important features of the emerging pattern. Were magmatic pulses independent of each other or were some nearly simultaneous over the entire SLIP? What are true dimensions of each area affected by a magmatic pulse? These and other questions can be comprehensively addressed only if much more new paleomagnetic data become available.

Acknowledgements

K.K.M. is in debt to A.V. Gerasimchuk, S.G. Mishenin and M.D. Tomshin who participated in sampling missions. We thank Nina Dvorova and Olga Krezhovskikh for paleomagnetic measurements. We highly appreciate the comments and suggestions by Anton Latyshev, Roman Veselovsky and Vladimir Pavlov on an earlier draft of this paper and the constructive reviews by Vincent Courtillot and an anonymous reviewer on the submitted manuscript. This study is a part of the ongoing research program funded by ALROSA Company. Support was also derived from the Russian Foundation of Basic Research, grants 12-05-00513 and 13-05-12030, Basic Research Programs #7 and #10 of the Earth Science Division, Russian Academy of Sciences and grant of the Government of the Russian Federation, Resolution #220, application # 2013-220-04-216.

Appendix A. Supplementary material

Supplementary material related to this article can be found online at <http://dx.doi.org/10.1016/j.epsl.2014.03.029>.

References

- Black, B.A., Elkins-Tanton, L.T., Rowe, M.C., Peate, I.U., 2012. Magnitude and consequences of volatile release from the Siberian Traps. *Earth Planet. Sci. Lett.* 317, 363–373.
- Bucur, I., 1994. The direction of the terrestrial magnetic field in France during the last 21 centuries. *Phys. Earth Planet. Inter.* 87, 95–109.
- Burgess, S.D., Bowring, S., Shen, S., 2014. High-precision timeline for Earth's most severe extinction. *Proc. Natl. Acad. Sci. USA*, published ahead of print February 10, 2014. <http://dx.doi.org/10.1073/pnas.1317692111>.
- Chenet, A., Fluteau, F., Courtillot, V., Gerard, M., Subbarao, K.V., 2008. Determination of rapid Deccan eruptions across the Cretaceous–Tertiary boundary using paleomagnetic secular variation: results from a 1200-m-thick section in the Mahabaleshwar escarpment. *J. Geophys. Res.* 113, B04101. <http://dx.doi.org/10.1029/2006JB004635>.
- Chenet, A.-L., Courtillot, V., Fluteau, F., Gerard, M., Quidelleur, X., Khadri, S.F.R., Subbarao, K.V., Thordarson, T., 2009. Determination of rapid Deccan eruptions across the Cretaceous–Tertiary boundary using paleomagnetic secular variation: 2. Constraints from analysis of eight new sections and synthesis for a 3500-m-thick composite section. *J. Geophys. Res.* 114 (B6), B06103. <http://dx.doi.org/10.1029/2008JB005644>.
- Cogné, J.P., 2003. PaleoMac: a Macintosh application for treating paleomagnetic data and making plate reconstructions. *Geochem. Geophys. Geosyst.* 4 (1), 1007. <http://dx.doi.org/10.1029/2001GC000227>.
- Courtillot, V., 1999. *Evolutionary Catastrophes: The Science of Mass Extinctions*. Cambridge Univ. Press, New York. 173 pp.
- Day, R., Fuller, M., Schmidt, V.A., 1977. Hysteresis properties of titanomagnetites: grain-size and compositional dependence. *Phys. Earth Planet. Inter.* 13, 260–267.
- Ernesto, M., Raposo, M.B., Marques, L., Renne, P., Diogo, L., Min, A., 1999. Paleomagnetism, geochemistry, and ⁴⁰Ar/³⁹Ar dating of the North-eastern Parana Magmatic Province: tectonic implications. *J. Geodyn.* 28, 321–340.
- Erwin, D.H., Bowring, S.A., Yogan, J., 2002. End-Permian mass extinction: a review. In: Koeberl, C., MacLeod, K.G. (Eds.), *Catastrophic Events and Mass Extinctions: Impacts and Beyond*. Boulder, Colorado. In: Geological Society of America. Special Papers, vol. 356, pp. 363–383.
- Foekistov, G.D., 1978. *Petrology and Conditions of Trap Sills Formation*. Nauka, Novosibirsk. 166 pp. (in Russian).

- Fisher, R.A., 1953. Dispersion on a sphere. *Proc. R. Soc. Lond. Ser. A* 217, 295–305.
- Gallet, Y., Pavlov, V.E., 1996. Magnetostratigraphy of the Moyero River section (northwestern Siberia): a constraint on the geomagnetic reversal frequency during the early Palaeozoic. *Geophys. J. Int.* 125, 95–105.
- Gallet, Y., Genevey, A., Le Goff, M., 2002. Three millennia of directional variation of the Earth's magnetic field in Western Europe as revealed by archeological artifacts. *Phys. Earth Planet. Inter.* 131, 81–89.
- Ganino, C., Arndt, N.T., 2009. Climate changes caused by degassing of sediments during the emplacement of large igneous provinces. *Geology* 37, 323–326.
- Gradstein, F.M., Ogg, J.G., Schmitz, M.D., Ogg, G.M. (Eds.), 2012. *The Geologic Time Scale 2012*. Elsevier, Amsterdam, 1144 pp.
- Gurevitch, E.L., Heunemann, C., Rad'ko, V., Westphal, M., Bachtadse, V., Pozzi, J.P., Feinberg, H., 2004. Palaeomagnetism and magnetostratigraphy of the Permian–Triassic northwest central Siberian Trap Basalts. *Tectonophysics* 379, 211–226.
- Hagstrum, J.T., Blinman, E., 2010. Archeomagnetic dating in western North America: an updated reference curve based on paleomagnetic and archeomagnetic data sets. *Geochem. Geophys. Geosyst.* 11, Q06009. <http://dx.doi.org/10.1029/2009GC002979>.
- Hargraves, R.B., Rehacek, J., Hooper, P.R., 1997. Palaeomagnetism of the Karoo igneous rocks in southern Africa. *S. Afr. J. Geol.* 100, 195–212.
- Heunemann, C., Krasa, D., Soffel, H.C., Gurevitch, E., Bachtadse, V., 2004. Directions and intensities of the Earth's magnetic field during a reversal: results from the Permo–Triassic Siberian trap basalts, Russia. *Earth Planet. Sci. Lett.* 218, 197–213.
- Ivanov, A.V., He, H., Yan, L., Ryabov, V.V., Shevko, A.Y., Paleskii, S.V., Nikolaeva, I.V., 2013. Siberian Traps large igneous province: evidence for two flood basalt pulses around the Permo–Triassic boundary and in the Middle Triassic, and contemporaneous granitic magmatism. *Earth-Sci. Rev.* <http://dx.doi.org/10.1016/j.earscirev.2013.04.001>.
- Johnson, C.L., Constable, C.G., Tauxe, L., Barendregt, R.W., Brown, L.L., Coe, R.S., Layer, P.W., Mejia, V., Opdyke, N.D., Singer, B.S., Staudigel, H., Stone, D.B., 2008. Recent investigations of the 0- to 5-Ma geomagnetic field recorded by lava flows. *Geochem. Geophys. Geosyst.* 9, Q04032. <http://dx.doi.org/10.1029/2007GC001696>.
- Kamo, S.L., Czamanske, G.K., Amelin, Y., Fedorenko, V.A., Davis, D.W., Trofimov, V.R., 2003. Rapid eruption of Siberian flood-volcanic rocks and evidence for coincidence with the Permian–Triassic boundary and mass extinction at 251 Ma. *Earth Planet. Sci. Lett.* 214, 75–91.
- Kirschvink, J.L., 1980. The least-square line and plane and the analysis of palaeomagnetic data. *Geophys. J. R. Astron. Soc.* 62, 699–718.
- Konstantinov, K.M., Mishenin, S.G., Kuzmenok, A.N., Tomshin, M.D., Gladkov, A.S., Vasuleva, A.E., 2007. Petro-magnetic heterogeneities of the Permian–Triassic traps in the Daldyn–Alakit area and their significance for diamond pipe prospecting. In: *Proceedings of Symposium "Paleomagnetism and Petro-magnetism: Theory, Practice, Experiment"*, Borok City, GEOS, pp. 63–69 (in Russian).
- Konstantinov, K.M., Gladkov, A.S., 2009. Petro-magnetic inhomogeneities in sintering zones of Permo–Triassic traps of Komsomolsk pipe deposits (Yakutsk diamond province). *Dokl. Earth Sci.* 427 (5), 880–886.
- Konstantinov, K.M., Tomshin, M.D., Gladkochub, D.P., Vasilieva, A.E., 2012. Petro-magnetic and petrogeochemical characteristics of Early Mesozoic basites in Udzha River basin (north-eastern Siberian Platform). *Lithosphere* 3, 80–98 (in Russian).
- Korobkov, I.G., Evstratov, A.A., Milshtein, E.D., 2013. *Basic Volcanostructures of Diamondiferous Structures in the East of the Tunguska Syncline*. STT Publishers, Tomsk (in Russian, 270 pp.).
- Latyshev, A.V., Veselovsky, R.V., Ivanov, A.V., Fetisova, A.V., Pavlov, V.E., 2013. Evidence of brief intense peaks of magmatic activity in the south Siberian platform (Angara–Taseeva Basin) as indicated by paleomagnetic studies. In: *Physics of the Solid Earth*, vol. 5, pp. 1–14.
- Lawrence, K.P., Tauxe, L., Staudigel, H., Constable, C.G., Koppers, A., McIntosh, W., Johnson, C.L., 2009. Paleomagnetic field properties at high southern latitude. *Geochem. Geophys. Geosyst.* 10, Q01005. <http://dx.doi.org/10.1029/2008GC002072>.
- Mankinen, E.A., Prevot, M., Gromme, G.S., Coe, R.S., 1985. The Steens Mountain (Oregon) geomagnetic polarity transition, 1. Directional history, duration of episodes, and rock magnetism. *J. Geophys. Res.* 90, 10393–10416.
- McFadden, P.L., McElhinny, M.W., 1988. The combined analysis of remagnetization circles and direct observations in palaeomagnetism. *Earth Planet. Sci. Lett.* 87, 161–172.
- McFadden, P., Merrill, R., McElhinny, M., 1988. Dipole/quadrupole family modeling of paleosecular variation. *J. Geophys. Res.* 93 (B10), 11583–11588.
- Merrill, R.T., McElhinny, M.W., McFadden, P.L., 1996. *The Magnetic Field of the Earth*. Acad. Press, San Diego, 527 pp.
- Moulin, M., Courtillot, V., Fluteau, F., Valet, J.-P., 2012. The “van Zijl” Jurassic geomagnetic reversal revisited. *Geochem. Geophys. Geosyst.* 13, Q03010. <http://dx.doi.org/10.1029/2011GC003910>.
- Paton, M.T., Ivanov, A.B., Fiorentini, M.L., McNaughton, N.J., Mudrovska, I., Demonterova, E.I., 2010. Late Permian and Early Triassic magmatic pulses in the Angara–Taseeva syncline, South Siberian Traps and their possible influence on the environment. *Russ. Geol. Geophys.* 51, 1012–1020.
- Pavlov, V.E., Gallet, Y., 1998. Upper Cambrian to Middle Ordovician magnetostratigraphy from the Kulumbe river section (northwestern Siberia). *Phys. Earth Planet. Inter.* 108, 49–59.
- Pavlov, V.E., Courtillot, V., Bazhenov, M.L., Veselovsky, R.V., 2007. Paleomagnetism of the Siberian traps: new data and a new overall 250 Ma pole for Siberia. *Tectonophysics* 443, 72–92.
- Pavlov, V.E., Fluteau, F., Veselovskiy, R.V., Fetisova, A.M., Latyshev, A.V., 2011. Secular geomagnetic variations and volcanic pulses in the Permian–Triassic traps of the Norilsk and Maymecha–Kotuy Provinces. *Physics of the Solid Earth* 47, 402–417.
- Raup, D.M., Sepkoski, J.J., 1982. Mass Extinctions in the Marine fossil record. *Science* 215, 1501–1503.
- Reichow, M.K., Pringle, M.S., Al'mukhamedov, A.I., Allen, M.B., Andreichev, V.L., Buslov, M.M., Davies, C.E., Fedoseev, G.S., Fitton, J.G., Inger, S., Medvedev, A.Y., Mitchell, C., Puchkov, V.N., Safonova, I.Y., Scott, R.A., Saunders, A.D., 2009. The timing and extent of the eruption of the Siberian Traps large igneous province: implications for the end-Permian environmental crisis. *Earth Planet. Sci. Lett.* 277, 9–20.
- Retallack, G.J., Jahren, A.H., 2008. Methane outbursts from igneous intrusion of coal at the Permian–Triassic boundary. *J. Geol.* 116, 1–20.
- Riisager, J., Riisager, P., Pedersen, A.K., 2003. Paleomagnetism of large igneous provinces: case-study from West Greenland, North Atlantic igneous province. *Earth Planet. Sci. Lett.* 214, 409–425.
- Suttie, N., Biggin, A.J., Holme, R., 2014. Correlation of palaeomagnetic directions constrains eruption rate of large igneous provinces. *Earth Planet. Sci. Lett.* 387, 4–9.
- Svensen, H., Planke, S., Chevallier, L., Malthe-Sorensen, A., Corfu, F., Jamtveit, B., 2007. Hydrothermal venting of greenhouse gases triggering Early Jurassic global warming. *Earth Planet. Sci. Lett.* 256, 554–566.
- Svensen, H., Planke, S., Polozov, A.G., Schmidbauer, N., Corfu, F., Podladchikov, Y.Y., Jamtveit, B., 2009. Siberian gas venting and the end-Permian environmental crisis. *Earth Planet. Sci. Lett.* 277, 490–500.
- Svensen, H., Corfu, F., Polteau, S., Hammer, Ø., Planke, S., 2012. Rapid magma emplacement in the Karoo Large Igneous Province. *Earth Planet. Sci. Lett.* 325–326, 1–9.
- Tarduno, J.A., Cottrell, R.D., Smirnov, A.V., 2002. The Cretaceous superchron geodynamo: observations near the tangent cylinder. *Proc. Natl. Acad. Sci. USA* 99, 14020–14025.
- Tauxe, L., Kent, D.V., 2004. A simplified statistical model for the geomagnetic field and the detection of shallow bias in paleomagnetic inclinations: was the ancient magnetic field dipolar? In: Channell, J.E.T., Kent, D.V., Lowrie, W., Meert, J.G. (Eds.), *Timescales of the Paleomagnetic Field*. In: *AGU Geophys. Monogr.*, vol. 135, pp. 101–116.
- Tomshin, M.D., Kopylova, A.G., Tyan, O.A., 2005. Petrochemical variability of traps at the eastern periphery of the Tungus Basin. *Russ. Geol. Geophys.* 46, 72–82.
- Vasiliev, Y.H., Zolotukhin, V.V., Feoktistov, G.D., Prusskaya, S.N., 2000. The volume estimates and the problem of origin of Permian–Triassic trap volcanism of the Siberian Platform. *Russ. Geol. Geophys.* 41, 1696–1705.
- Veselovsky, R.V., Gallet, Y., Pavlov, V.E., 2003. Paleomagnetism of traps in the Podkammennaya Tunguska and Kotuy River valleys: implications for the post-Paleozoic relative movements of the Siberian and East European platforms. *Physics of the Solid Earth* 39, 856–871.
- Veselovsky, R.V., Konstantinov, K.M., Latyshev, A.V., Fetisova, A.M., 2012. Paleomagnetism of the Trap intrusive bodies in Arctic Siberia: geological and methodical Implications. *Physics of the Solid Earth* 48, 738–750.
- Wignall, P.B., 2001. Large igneous provinces and mass extinctions. *Earth-Sci. Rev.* 53, 1–33.
- Xie, S.C., Pancost, R.D., Huang, J.H., Wignall, P.B., Yu, J.X., Tang, X.Y., et al., 2007. Changes in the global carbon cycle occurred as two episodes during the Permian–Triassic crisis. *Geology* 35, 1083–1086.
- Zijderveld, J.D.A., 1967. AC demagnetization of rocks: analysis of results. In: Collinson, D.W., Creer, K.M. (Eds.), *Methods in Paleomagnetism*. Elsevier, Amsterdam, pp. 254–286.
- Zolotukhin, V.V., Al'mukhamedov, A.I., 1988. Traps of the Siberian platform. In: Macdougall, J.D. (Ed.), *Continental Flood Basalts*. Kluwer, Dordrecht, Netherlands, pp. 273–310.